Mechanisms Involved in Synergistic Anticancer Immunity of Anti-4-1BB and Anti-CD4 Therapy

Beom K. Choi,[1] Young H. Kim,[1] Woo J. Kang,[1] Sun K. Lee,[1] Kwang H. Kim,[1] Su M. Shin,[1] Wayne M. Yokoyama,[2] Tae Y. Kim,[1] and Byoung S. Kwon[1,3,4]

[1]The Immunomodulation Research Center, University of Ulsan, Ulsan, Korea; [2]Howard Hughes Medical Institute, Washington University School of Medicine, St. Louis, Missouri; [3]LSU Eye Center, Louisiana State University Health Sciences Center, New Orleans, Louisiana; and [4]National Cancer Center, Goyang-Si, Gyeonggi-do, Korea

Abstract

Anti-4-1BB–mediated anticancer effects were potentiated by depletion of $CD4^+$ cells in B16F10 melanoma-bearing C57BL/6 mice. Anti-4-1BB induced the expansion and differentiation of polyclonal tumor-specific $CD8^+$ T cells into IFN-γ–producing $CD11c^+CD8^+$ T cells. The $CD4^+$ cell depletion was responsible for facilitating immune cell infiltration into tumor tissues and removing some regulatory barriers such as T regulatory and indoleamine-2,3-dioxygenase $(IDO)^+$ dendritic cells. Both monoclonal antibodies (mAb) contributed to the efficient induction of MHC class I molecules on the tumor cells *in vivo*. The effectors that mediated the anti-4-1BB effect were $NKG2D^+KLRG1^+CD11c^+CD8^+$ T cells that accumulated preferentially in the tumor tissues. Blocking NKG2D reduced the therapeutic effect by 20% to 26%, which may indicate that NKG2D contributes partially to tumor killing by the differentiated $CD8^+$ T cells. Our results indicate that the combination of the two mAbs, agonistic anti-4-1BB and depleting anti-CD4, results in enhanced production of efficient tumor-killing CTLs, facilitation of their infiltration, and production of a susceptible tumor microenvironment. [Cancer Res 2007;67(18):8891–9]

Introduction

Immunotherapy is an approach to treating intractable diseases such as tumors, autoimmune diseases, transplantation rejection, and chronic infections by enhancing, suppressing, or modifying the immune system. One of the goals of immunotherapy is to achieve selective immune enhancement or suppression without deleterious effects on the global immunity of the host. 4-1BB is induced on the T-cell surface in an antigen-specific manner and directs antigen-specific immune responses; this provides a means to achieve such selectivity when it is used in immunotherapy (1, 2).

The efficacy of agonistic anti-4-1BB in tumor therapy has been well documented. Its therapeutic effects are mediated by enhancing natural killer (NK) and $CD8^+$ T-cell activation and IFN-γ production (3–6). In a mouse melanoma model, however, injection of anti-4-1BB only partially suppressed B16-F10 subcutaneous tumors, although it preferentially increased the $CD8^+$ T-cell response and IFN-γ production (6). To overcome some of the barriers that may inhibit anti-4-1BB–mediated anticancer effects, we have tested the efficacy of various reagents in combination with anti-4-1BB in B16 melanoma-bearing mice. Among the reagents, depleting anti-CD4 was the most efficient at increasing the effect of anti-4-1BB–mediated tumor therapy.

We describe here the therapeutic effect of an agonistic anti-4-1BB in combination with a depleting anti-CD4 monoclonal antibody (mAb) in a B16-F10 melanoma model. We found that anti-4-1BB treatment resulted in the polyclonal expansion and differentiation of $CD8^+$ T cells into effective tumor killers. $CD4^+$ T-cell depletion facilitated the infiltration of immune cells into the tumors and removed regulatory barriers such as T regulatory (Treg) and IDO^+ dendritic cells. Both mAbs contributed to creating a $CD8^+$ T-susceptible tumor microenvironment by inducing class I molecules on the surface of the melanoma cells.

Materials and Methods

Mice. IFN-γ–deficient (GKO) and Rag2-deficient C57BL/6 mice (6–8 weeks old) were purchased from The Jackson Laboratory. All mice were maintained under specific pathogen-free conditions in the Immunomodulation Research Center. The animal studies were approved by the Institutional Animal Care and Use Committee of the University of Ulsan.

Antibodies and peptides. Anti-m4-1BB hybridoma cells (3E1) were a gift from Dr. Robert Mittler (Emory University, Atlanta, GA) and the anti-NKG2D mAb (C7) was described previously (7). The anti-mCD4 (GK1.5) and anti-NK1.1 (PK136) hybridomas were obtained from American Type Culture Collection. The anti-mouse indoleamine 2,3-dioxygenase (IDO) mAb (mIDO-1) was generated in our laboratories. The following mAbs were purchased from BD PharMingen: FITC- or phycoerythrin (PE)-Cy5-anti-CD8α (53-6.7), FITC- or PE-Cy5-anti-CD8β (Ly-3.2, 53-5.8), PE- or PE-Cy5-anti-CD4 (H129.19), FITC-anti-CD25, FITC- or PE-anti-CD11c (HL3), PE-anti-CD11b (M1/70), FITC- or PE-anti-CD3 (145-2C11), PE-anti-B220 (RA3-6B2), PE-anti-NK1.1 (PK136), PE-anti-IFN-γ (XMG1.2), purified anti-CD16/CD32 (2.4G2), biotin-anti-CD40 (3/23), and biotin-anti-B220 (RA3-6B2). FITC- or PE-anti-NKG2D (CX5), PE-Cy5-anti-TCRβ biotin-anti F4/80 (BM8), biotin-anti-KLRG1 (MAFA, 2F1), and FITC- or PE-streptavidin were purchased from eBioscience. FITC- or PE-anti-PDCA-1 (JF05-1C2.4.1) were obtained from Miltenyi Biotec. Tumor peptides were synthesized by Peptron: mgp100 (ITDQVPFSV), mMAGE-A1 (HNTQYCNL), mTyrosinase (FMDGTMSQV), and mTRP2 (VYDFFVWL).

Treatments. Mice were challenged s.c. on the back with 4×10^5 B16-F10 melanoma cells. For preventative therapy, mice were injected i.p. with 100 μg anti-4-1BB and/or 400 μg anti-CD4 every 5 days. To deplete NK cells, tumor-bearing mice received 400 μg anti-NK1.1 i.p. every 5 days. For NKG2D blocking, mice were given 500 μg anti-NKG2D every 5 days. For assessing the antitumor effects of delayed therapy, mice were treated as described above when tumors were 3 to 5 mm in diameter.

Proliferation assay *in vivo*. Tumor-draining lymph nodes (TDLN) were harvested 1 h after injecting 1 mg BrdUrd into tumor-bearing mice. The cells were surface-stained with PE-conjugated anti-CD4, anti-CD8, or anti-B220 alone, or with PE-conjugated anti-CD11c and PE-Cy5–conjugated anti-CD8, and then fixed, permeabilized, and intracellularly stained with FITC-conjugated anti-BrdUrd (BD Bioscience).

Note: Supplementary data for this article are available at Cancer Research Online (http://cancerres.aacrjournals.org/).

B.K. Choi and Y.H. Kim contributed equally to this work.

Requests for reprints: Byoung S. Kwon, The Immunomodulation Research Center, University of Ulsan, Ulsan 680-749, Korea. Phone: 82-52-259-2874; Fax: 82-52-259-2740; E-mail: bskwon@mail.ulsan.ac.kr.

doi:10.1158/0008-5472.CAN-07-1056

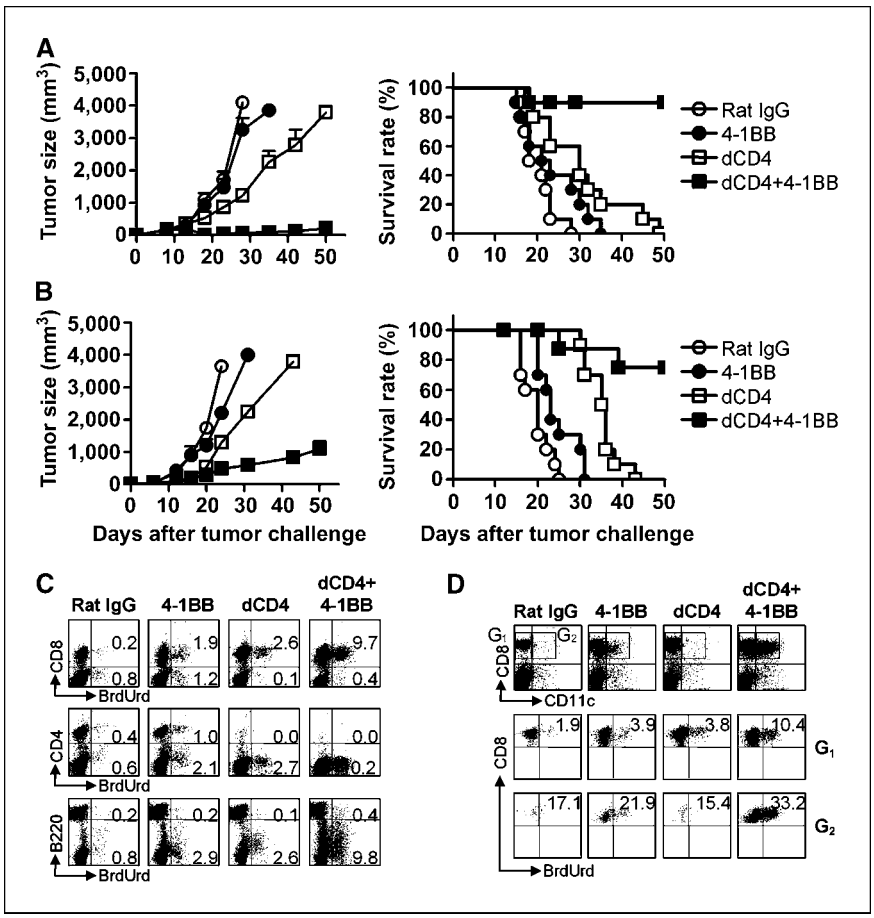

Figure 1. Antitumor effects of combined therapy with anti-4-1BB and anti-CD4 mAb. C57BL/6 mice were challenged s.c. on the back with 4×10^5 B16-F10 melanoma cells. The mice were also injected i.p. with 100 μg anti-4-1BB (3E1) and/or 400 μg anti-CD4 (GK1.5), or 100 μg rat IgG as a control, five times every 5 d (*A*). For delayed therapy, B16-F10 melanoma-bearing mice were treated in the same way starting on PI day 6 when the tumors were 3 to 5 mm in diameter (*B*). They were monitored every day, and tumor volume and survival were measured as described above. To assess BrdUrd incorporation *in vivo*, the mice were i.p. injected with 1 mg BrdUrd on PI day 12. One hour after the BrdUrd labeling, TDLN cells were harvested and surface-stained with PE-conjugated anti-CD8, anti-CD4, or anti-B220 mAb, and then stained intracellularly with FITC-conjugated BrdUrd mAb (BD Bioscience; *C*). For detailed analysis of BrdUrd incorporation into the $CD8^+$ T cells, TDLN cells were surface-stained with PE-conjugated anti-CD11c and PE-Cy5-conjugated anti-CD8 mAbs. Following intracellular staining of BrdUrd, $CD11c^-CD8^+$ T, and $CD11c^+CD8^+$ T cells were separately analyzed by gating on a CD8 versus CD11c dot plot (*D*). *Points,* means (n = 10 mice per group in *A* and *B* and n = 5 mice per group in *C* and *D*); *bars,* SD. The results are representative of five independent experiments.

Flow cytometry. Cells were incubated with the Fc blocker 2.4G2 for 10 min at 4°C and stained with specific antibodies to surface markers. The expression of MHC class I or IFN-γR on B16-F10 melanoma were determined by staining with PE-conjugated anti-H-$2K^b$, H-$2D^b$, or IFN-γR as well as an FITC-conjugated anti-CD3, anti-CD4, anti-CD8, anti-CD11c, anti-B220, anti-F4/80, anti-NK1.1, or anti-Gr-1. All samples were analyzed on a FACScalibur (BD Bioscience).

Absolute cell numbers. Cells were stained with anti-CD3, anti-CD4, anti-CD8, anti-CD11b, anti-CD11c, or anti-NK1.1. Percentage of lymphocyte was determined by a flow cytometry. The absolute number of each population was calculated by multiplying the total number of viable cells by the percentage determined.

Cytokines. Tumor or spleen tissues were weighed and homogenized in PBS-containing protease inhibitors, and the supernatants were collected by centrifugation. The cytokines in the supernatants were quantified using a cytometric bead array kit (BD Bioscience).

CD107 mobilization assay. CD107 mobilization was determined as described (8) on TDLN-derived effector cells in the presence of tumor antigen-pulsed EL4 cells on propidium iodide (PI) day 15.

Tumor-infiltrating lymphocytes. The single-cell suspensions of tumor tissue were layered over 36% and 63% Percoll gradient, and centrifuged for 45 min at 400 × *g* at room temperature. Tumor-infiltrating lymphocytes (TIL) were recovered from the interface between the 36% and 63% Percoll layers, washed, and analyzed by flow cytometry (6).

Adoptive transfer of $CD8^+$ T cells. $CD8^+$ T cells from naïve C57BL/6 were adoptively transferred i.v. into $Rag2^{-/-}$ mice at 2×10^7 cells per mouse. The mice received the B16-F10 melanoma cells and antibodies as described above. On PI day 15, TDLNs and tumor tissue were collected from each group of mice and stained with PE-conjugated anti-CD11c and PE-Cy5–conjugated anti-CD8β mAbs to determine the proportion of $CD11c^+CD8^+$ T cells.

Confocal microscopy. Sections of tumor tissue (6 μm thickness) were stained with PE-conjugated anti-H-$2K^b$, anti-H-$2K^d$, or anti-IDO, and mounted with Prolong Anti-fade (Molecular Probes). All sections were viewed and photographed using a laser-scanning confocal fluorescence microscope system (Fluoview FV500).

IDO in dendritic cells. $CD11c^+$ dendritic cells were purified from the T cell–depleted TDLN cells using CD11c-microbeads (Miltenyi Biotec). Proteins were extracted with lysis buffer and subjected to Western blotting with anti-IDO.

Results

$CD4^+$ cell depletion enhances the antitumor response to anti-4-1BB. To enhance the 4-1BB–mediated antitumor CTL response, we tested a variety of reagents such as blocking anti-CTLA-4, blocking PD-1, depleting anti-CD25, or depleting anti-CD4 mAbs in combination with anti-4-1BB. A synergistic antitumor effect was observed when the anti-4-1BB was used in combination with depleting anti-CD4 in the B16-F10 melanoma model. Anti-4-1BB or anti-CD4 treatment by themselves slightly suppressed tumor growth and somewhat prolonged survival time (Fig. 1*A*). On the other hand, coadministration of anti-4-1BB and anti-CD4 not only successfully inhibited tumor growth but also increased survival (Fig. 1*A*). In this case, the mice survived for >50 days after inoculation of the B16-F10 melanoma, and the suppression of tumor growth was sustained. Tumor-bearing mice were also treated with anti-4-1BB and/or anti-CD4 from day 6 after tumor inoculation when the tumors were 3 to 5 mm in diameter. Anti-4-1BB or anti-CD4 mAb alone resulted in slight suppression of tumor

growth and somewhat delayed the death of the tumor-bearing mice (Fig. 1*B*). Again, coadministration of anti-4-1BB and anti-CD4 had a profound suppressing effect on tumor growth and increased the survival of the tumor-bearing mice (Fig. 1*B*; Supplementary Fig. S1).

Because $CD8^+$ T cells are primarily responsible for successful tumor therapy (9–11), we first assessed the *in vivo* proliferation of $CD8^+$ T cells in anti-4-1BB– and/or anti-CD4–treated mice. Proliferating cells obtained from TDLNs (inguinal lymph nodes) were identified by labeling the mice with BrdUrd on PI day 12. There were only a few proliferating $CD8^+$, $CD4^+$ T, and $B220^+$ B cells (<0.5%) in mice treated with control rat antibody. Anti-4-1BB treatment preferentially increased the proliferation of $CD8^+$ T cells (1.9 ± 0.45%) over $CD4^+$ T (1.0 ± 0.29%) or B cells (0.2 ± 0.1%). Anti-CD4 treatment also enhanced the proliferation of $CD8^+$ T cells (2.6 ± 0.5%), but not B cells (<0.1%). However, coadministration of anti-4-1BB with anti-CD4 resulted in the presence of a large number of proliferating $CD8^+$ T cells; their proportion (9.7 ± 2.3%) was 5.1-fold higher than after anti-4-1BB treatment, and 3.7-fold higher than after anti-CD4 treatment (Fig. 1*C*).

As we previously reported (2), anti-4-1BB treatment induces a subset of $CD8^+$ T cells, namely $CD11c^+CD8^+$ T cells, in an antigen-specific and 4-1BB–dependent manner. Therefore, we tested whether the proliferating $CD8^+$ T cells included $CD11c^+CD8^+$ T cells. After staining the same BrdUrd-labeled lymphocytes with anti-CD11c, and with anti-CD8β to exclude $CD8\alpha\alpha^+$ dendritic cells, $CD11c^-CD8^+$ and $CD11c^+CD8^+$ T cells were separately gated on a CD8 versus CD11c dot plot and the proportion of proliferating cells in each population was determined. Of the $CD11c^+CD8^+$ T cells, 33.2 ± 4.7% were proliferating cells compared with only 10.4 ± 2.9% of the $CD11c^-CD8^+$ T cells (Fig. 1*D*).

Taken together, these results indicate that the strong antitumor immune response evoked by coadministration of anti-4-1BB and anti-CD4 results from robust proliferation of $CD11c^+CD8^+$ T cells.

$CD4^+$ cell depletion enhances the anti-4-1BB–mediated expansion and differentiation of $CD8^+$ T cells. We next analyzed the effect of anti-CD4 on the anti-4-1BB–mediated $CD8^+$ T-cell response. We prepared TDLN cells from the four groups of mice 15 days after tumor challenge and determined the percentages and absolute numbers of $CD11c^+CD8^+$ T cells and IFN-γ–producing $CD8^+$ T cells. Anti-4-1BB treatment preferentially increased the number of $CD8^+$ T cells and eventually reversed the ratio of $CD4^+$ to $CD8^+$ T cells (data not shown). Anti-4-1BB increased the absolute number of $CD8^+$ T cells 2.5-fold in the TDLNs, and anti-CD4 increased it 4.5-fold, compared with control IgG (Fig. 2*A, bottom left*). The combination therapy produced the highest number of $CD8^+$ T cells: a 7- to 9-fold increase over the control IgG-treated group. Anti-4-1BB was, however, more effective in inducing

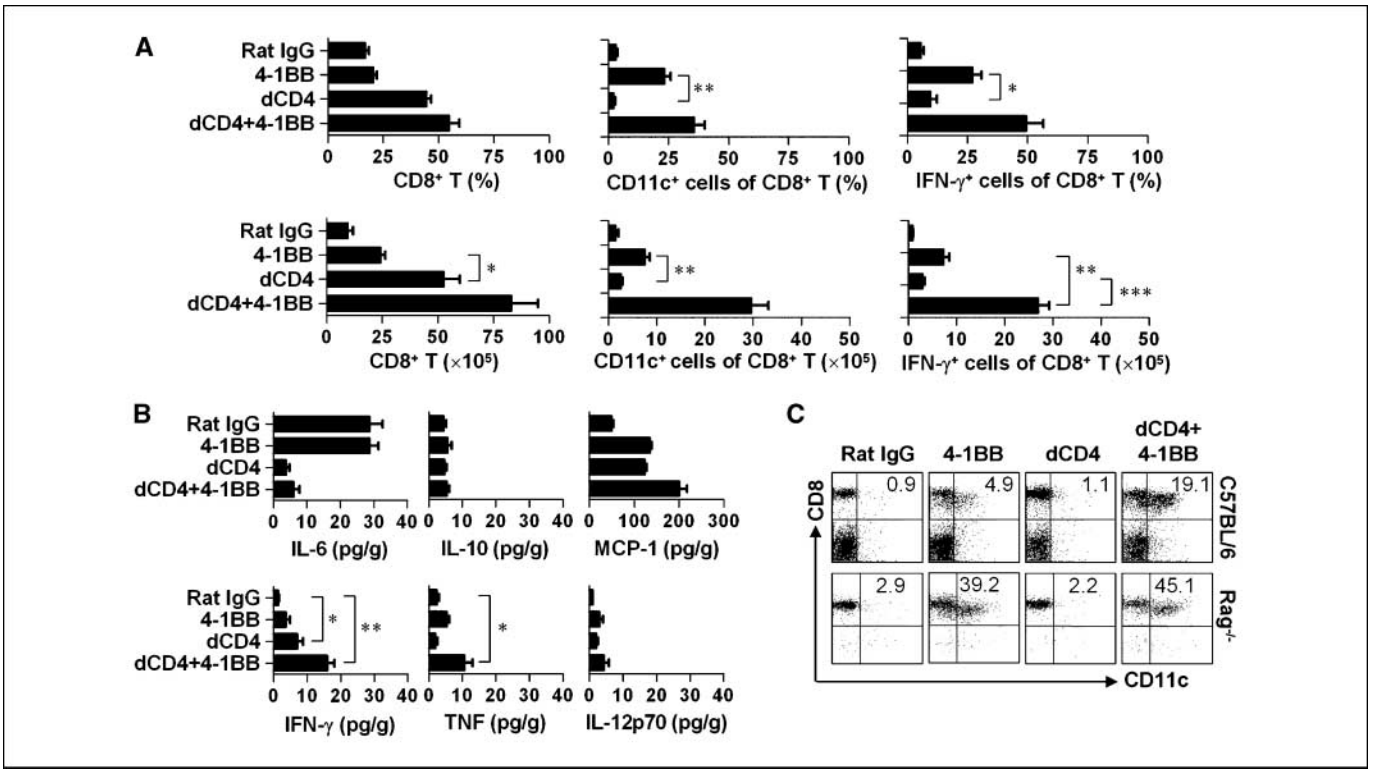

Figure 2. Combination therapy with anti-4-1BB and anti-CD4 enhances the expansion and differentiation of $CD8^+$ T cells. Tumor-challenged mice were treated with antibodies as described above. *A,* the percentages of total, IFN-γ^+, or $CD11c^+$ $CD8^+$ T cells in the TDLNs were determined by fluorescence-activated cell sorting on PI day 15 (*A, top*). TDLN cells were stimulated *in vitro* with 50 ng/mL phorbol 12-myristate 13-acetate and 500 ng/mL ionomycin in the presence of Brefeldin A for 6 h, incubated with 2.4G2 for 10 min at 4°C, stained with FITC-labeled anti-CD8 or anti-CD4, fixed, permeabilized with a Cytofix kit, incubated with PE-anti-IFN-γ, and analyzed by FACS. Absolute numbers were calculated by multiplying the percentages measured by flow cytometry by the total number of viable cells (*A, bottom*). *B,* tumor tissues were collected from mice on PI day 15 and homogenized. The supernatant was collected and assayed with a cytometric bead array kit (BD Bioscience). Data shown are cytokine concentrations per gram of tumor tissue. *C,* $Rag2^{-/-}$ mice that received 2×10^7 of wild-type $CD8^+$ T cells and C57BL/6 mice were inoculated with B16-F10 melanoma cells and antibodies as described above. Lymphocytes were collected from TDLNs and tumor tissue on PI day 15 and stained with PE-Cy5–conjugated anti-CD8β and PE-conjugated anti-CD11c mAbs. *Columns,* mean (n = 10 mice per group in *A* and *B* and n = 5 mice per group in *C*); *bars,* SD.*, $P < 0.05$; **, $P < 0.01$. All results are representative of three independent experiments.

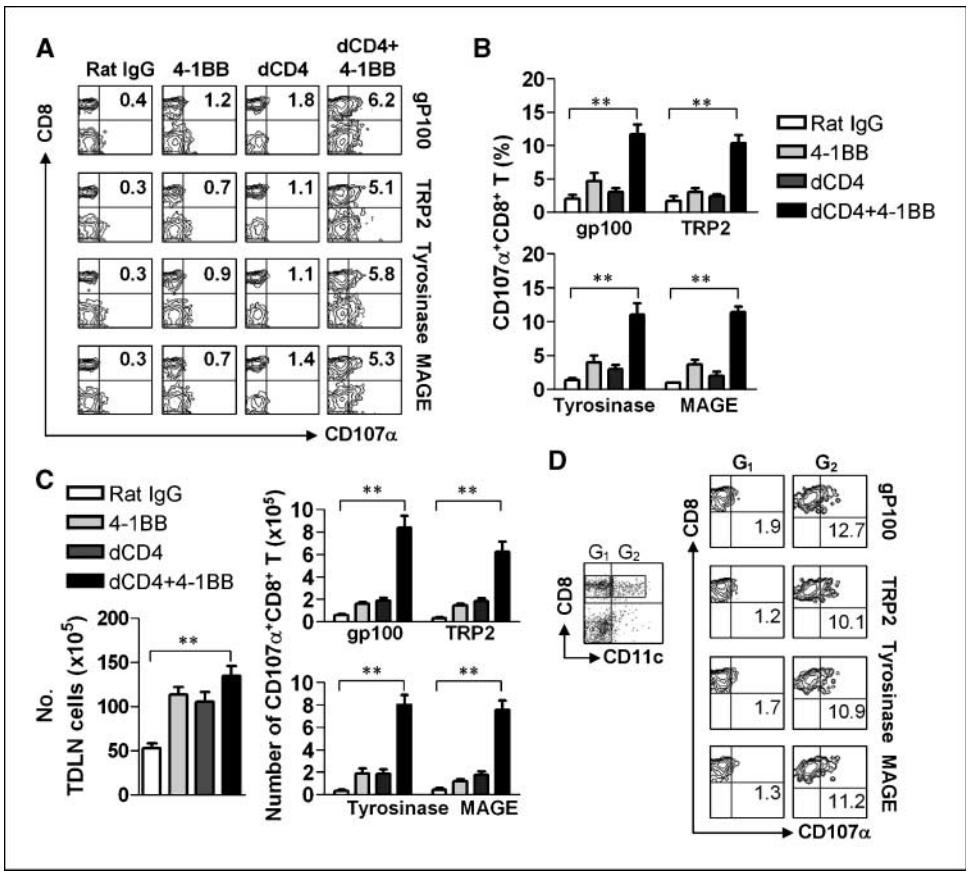

Figure 3. Combination therapy results in polyclonal expansion of tumor-specific CTL. Tumor-bearing mice were treated with antibodies as described above. TDLN cells were cocultured with EL4 cells pulsed with each peptide (gp100, TRP2, tyrosinase, and MAGE) at a 2:1 ratio in the presence of 3 μmol/L monensin and 1 μg CD107α (anti-LAMP-1) mAb for 5 h. Cell-to-cell conjugates were disrupted by washing the cells with PBS with 0.02% azide and 0.5 mmol/L EDTA. CD107α-positive cells were detected by staining the cells with anti-rat IgG-FITC as well as PE-conjugated anti-CD11c and PE-Cy5–conjugated anti-CD8 mAbs. All samples were subsequently analyzed by FACS. *A,* representative data acquired by flow cytometry. *B,* average percentage of CD107α-positive cells among the $CD8^+$ T cells in three independent experiments. *C,* absolute number of $CD107\alpha^+CD8^+$ T cells calculated from (*B*). *D,* CD107α-positive cells among the $CD11c^-CD8^+$ and $CD11c^+CD8^+$ T cells from the anti-4-1BB plus anti-CD4–treated group. *Columns,* means (n = 10 mice per group; *, $P < 0.05$; **, $P < 0.01$); *bars,* SD. Results are representative of three independent experiments.

$CD11c^+CD8^+$ T cells than anti-CD4 (23.3 ± 2.6% versus 2.3 ± 0.49% of $CD8^+$ T cells). The combination of the two mAbs resulted in a synergistic increase in the double-positive cells (35.7 ± 4.3% of $CD8^+$ T cells; Fig. 2*A, top middle*). The absolute number of $CD11c^+CD8^+$ T cells was increased ~50-fold by the combination therapy compared with the control IgG- or anti-CD4–treated mice, and ~10-fold compared with the anti-4-1BB–treated mice (Fig. 2*A, bottom middle*). IFN-γ production was particularly noticeable because the combination therapy increased IFN-γ–producing $CD8^+$ T cells >50-fold and 8.5-fold compared with the control IgG- and anti-CD4–treated mice, respectively (Fig. 2*A, right*). It also produced ~3-fold more IFN-γ–producing $CD8^+$ T cells than anti-4-1BB alone. In the anti-4-1BB–treated mice, $CD4^+$ T cells also induced IFN-γ production (data not shown). As shown in Fig. 2*A* (*top right*), almost 50% of the $CD8^+$ T cells produced IFN-γ in the combination therapy and ~28% in the anti-4-1BB treatment. Although anti-CD4 treatment markedly increased the number of $CD8^+$ T cells in the TDLNs, the ratio of IFN-γ–producing $CD8^+$ T cells was comparable with that in the control IgG-treated mice (Fig. 2*B, top right*), indicating that anti-CD4 is not involved in $CD8^+$ T-cell differentiation. However, the anti-4-1BB treatment not only increased the number of $CD8^+$ T cells, but also promoted the differentiation of $CD8^+$ and $CD4^+$ T cells into IFN-γ–producing effector T cells (Supplementary Fig. S2).

Due to the enhanced $CD8^+$ T response by anti-4-1BB treatment, we determined the levels of cytokines in tumor tissues and in the spleen. In tumor tissues, anti-4-1BB or anti-CD4 increased the production of proinflammatory cytokines such as IFN-γ, tumor necrosis factor-α (TNF-α), IL-12p70, and MCP-1 with the highest increase in the combination therapy. IL-6 and IL-10 levels were decreased or not altered by the above treatments (Fig. 2*B*). In the spleen, the level of IFN-γ was significantly increased by the anti-4-1BB or combination therapy. TNF-α production was enhanced only by the anti-4-1BB treatment. No changes in the levels of other cytokines were statistically significant (Supplementary Fig. S3). These results suggest that anti-4-1BB and anti-CD4 treatments promote type 1 cellular immune responses in the tumor tissues.

To assess the involvement of anti-4-1BB and anti-CD4 in the differentiation of $CD8^+$ T cells into $CD11c^+CD8^+$ T cells more stringently, purified $CD8^+$ T cells were adoptively transferred to syngeneic $Rag2^{-/-}$ and C57BL/6 mice; melanomas were induced and the mice were exposed to the four different regimens; control IgG, anti-4-1BB, anti-CD4, and anti-4-1BB plus anti-CD4. The formation of $CD8^+$ T cells was mainly dependent on anti-4-1BB, and the depletion of $CD4^+$ cells had almost no effect (Fig. 2*C*).

Taken together, our findings indicate that anti-4-1BB treatment was able to induce the proliferation and differentiation of $CD8^+$ T cells, as well as the production of cytokines, including IFN-γ, TNF-α, MCP-1, and IL-12p70. On the other hand, anti-CD4 treatment markedly increased the number of $CD8^+$ T cells, but did not promote the formation of IFN-γ–producing cells. Therefore, anti-CD4 treatment tended to induce the proliferation of $CD8^+$ T cells rather than their differentiation into effector cells. Anti-4-1BB treatment eventually generated more IFN-γ–producing $CD11c^+CD8^+$ T cells than anti-CD4 (Fig. 2*A*). These results indicate that depletion of $CD4^+$ cells facilitates and potentiates the anti-4-1BB–mediated expansion and differentiation of $CD8^+$ T cells.

CD11c$^+$CD8$^+$ T cells are effectors of anti-4-1BB–mediated tumor suppression. We tested whether the combination therapy increased the number of tumor-associated antigen (TAA)–specific CTLs. We used four different TAAs: gp100, tyrosinase-related protein 2 (TRP2), tyrosinase, and melanoma-associated Ag A1 (MAGE-A1) to determine whether the 4-1BB–mediated expansion of CTLs is polyclonal and whether the expansion involves all tumor-specific CTLs, not just certain antigen-specific CTLs. Tumor antigen–specific CTLs were enumerated by assessing the number of CD107α (lysosomal-associated membrane protein-1)–positive CD8$^+$ T cells during coculture with TAA peptide-pulsed target cells (8). Lymphocytes were prepared from the TDLNs of the four groups of mice on PI day 15 and cocultured with gp100, TRP2, tyrosinase, or MAGE-A1 peptide-pulsed EL4 cells at a 2:1 ratio in the presence of monensin and anti-CD107α mAb for 5 h. Flow cytometric analysis showed that CD107α-positive cells were barely detectable on the surface of CD8$^+$ T cells from the rat IgG-treated mice (0.3 ~ 0.4%) but were present against each of the four TAAs at a level of 0.7% to 1.8% in the anti-4-1BB– or anti-CD4–treated mice. However, in the combination therapy group, >5% of the total cells were CD107α$^+$CD8$^+$ T cells against each of four TAAs (Fig. 3*A*). Anti-4-1BB treatment seemed to be more effective than anti-CD4 for producing antigen-specific killers (Fig. 3*B*). In the combination therapy, the proportion of CD107α-positive cells to each of four TAAs among the CD8$^+$ T cells reached around 12% (Fig. 3*B*). Specific lysis assays yielded results in agreement with the observed CD107α$^+$CD8$^+$ T-cell frequencies (Supplementary Fig. S4).

The absolute numbers of CTLs in the TDLNs specific for each tumor antigen were determined (Fig. 3*C*). In the anti-4-1BB– or anti-CD4–treated mice, the frequency of antigen-specific CTLs was 3- to 10-fold higher than in the control IgG-treated mice, whereas the combination therapy increased the number of CTLs >40-fold against all the TAAs tested. Reanalysis of the CD107α$^+$ cells in the CD11c$^-$CD8$^+$ and CD11c$^+$CD8$^+$ T subsets of the mice given the combination therapy again supported the hypothesis that CD11c$^+$CD8$^+$ T cells are the effectors of anti-4-1BB–based tumor therapy because most of the CD107α$^+$CD8$^+$ T cells were restricted to the CD11c$^+$CD8$^+$ T cells (Fig. 3*D*).

We conclude therefore that the suppression of tumor growth by anti-4-1BB treatment is primarily the consequence of the extensive increase of tumor-specific CTLs that express CD11c molecules on their surface, and that the CTLs expanded by anti-4-1BB treatment are polyclonal. Depleting CD4$^+$ cells again synergistically enhanced the anti-4-1BB–mediated expansion of CTLs.

Selective accumulation of CD11c$^+$CD8$^+$ T cells in tumor tissue. We examined the phenotype of the CD8$^+$ T cells that infiltrated the tumor tissues on PI day 15. There were only a few CD8$^+$ T cells among the TILs in the control IgG-treated mice. However, anti-4-1BB treatment not only increased the infiltration of CD8$^+$ T cells, but most of the CD8$^+$ TILs were CD11c$^+$CD8$^+$ T cells. Anti-CD4 treatment alone increased the infiltration of various types of immune cells, and, unexpectedly, 17.1% of the TILs were CD11c$^+$CD8$^+$ T cells, although this cell population was rarely detected in TDLNs. It seems that CD11c$^+$CD8$^+$ T cells are generated during normal immune responses and rapidly migrate to target tissues. By combining anti-4-1BB with anti-CD4 mAb, the infiltration of CD8$^+$CD11c$^+$ T cells was markedly increased, and they became to represent nearly 80% of all the TILs (Fig. 4*A*).

When we calculated the absolute numbers of each cell population in tumor tissue, each type of treatment yielded a distinct profile of cell infiltration. Anti-CD4 seemed to greatly facilitate the infiltration of a variety of immune cells, including CD3$^+$ T and NK cells, monocytes/macrophages, and dendritic cells, whereas anti-4-1BB treatment preferentially increased the infiltration of CD8$^+$ T cells, particularly CD8$^+$CD11c$^+$ T cells (Fig. 4*B*). The absolute number of tumor-infiltrating immune cells in the anti-CD4 group was 8- and 4-fold more than that in the control IgG- and anti-4-1BB–treated groups, respectively, indicating that CD4$^+$ cells

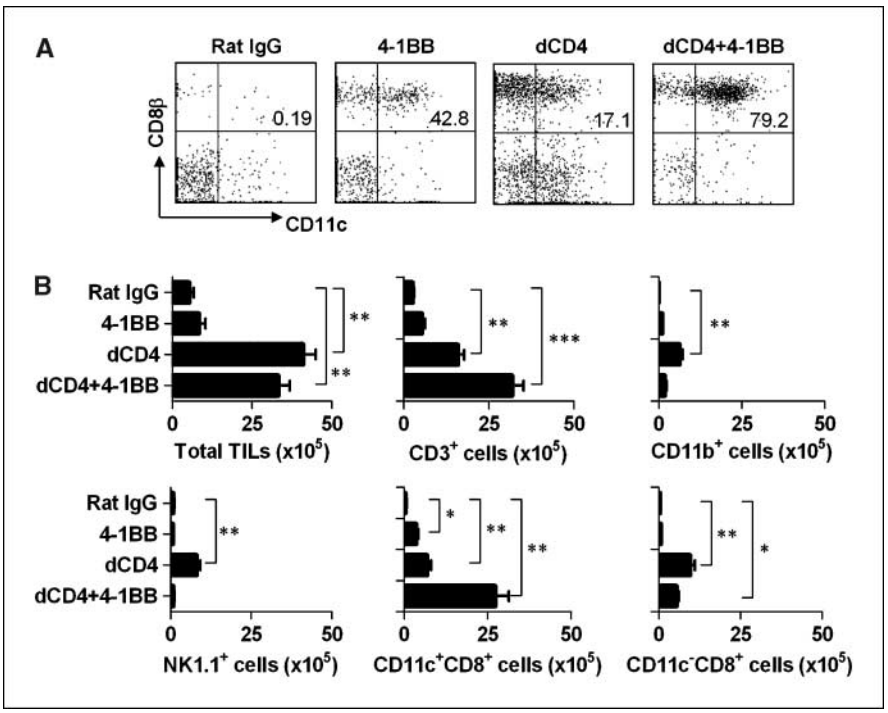

Figure 4. Preferential accumulation of CD11c$^+$CD8$^+$ T cells in tumor tissue. Tumor-bearing mice were treated with antibodies as described above. Tumors were collected, cut into pieces, and resuspended in DMEM supplemented with 2% fetal bovine serum and 1.5 mg/mL of collagenase D for 40 min at 37°C. TILs were enriched by 36%/63% Percoll gradient centrifugation on PI day 15. *A,* staining of TILs with PE-conjugated anti-CD8 and FITC-conjugated anti-CD11c mAb. *B,* TILs were stained with anti-CD3 and anti-NK1.1, anti-CD11b, or anti-CD8, and anti-CD11c mAbs. The absolute numbers of each population were calculated by multiplying the percentage measured by flow cytometry by the total number of viable cells. *Columns,* mean (n = 5 mice per group; *, $P < 0.05$; **, $P < 0.01$; ***, $P < 0.001$); *bars,* SD. Results are representative of four independent experiments.

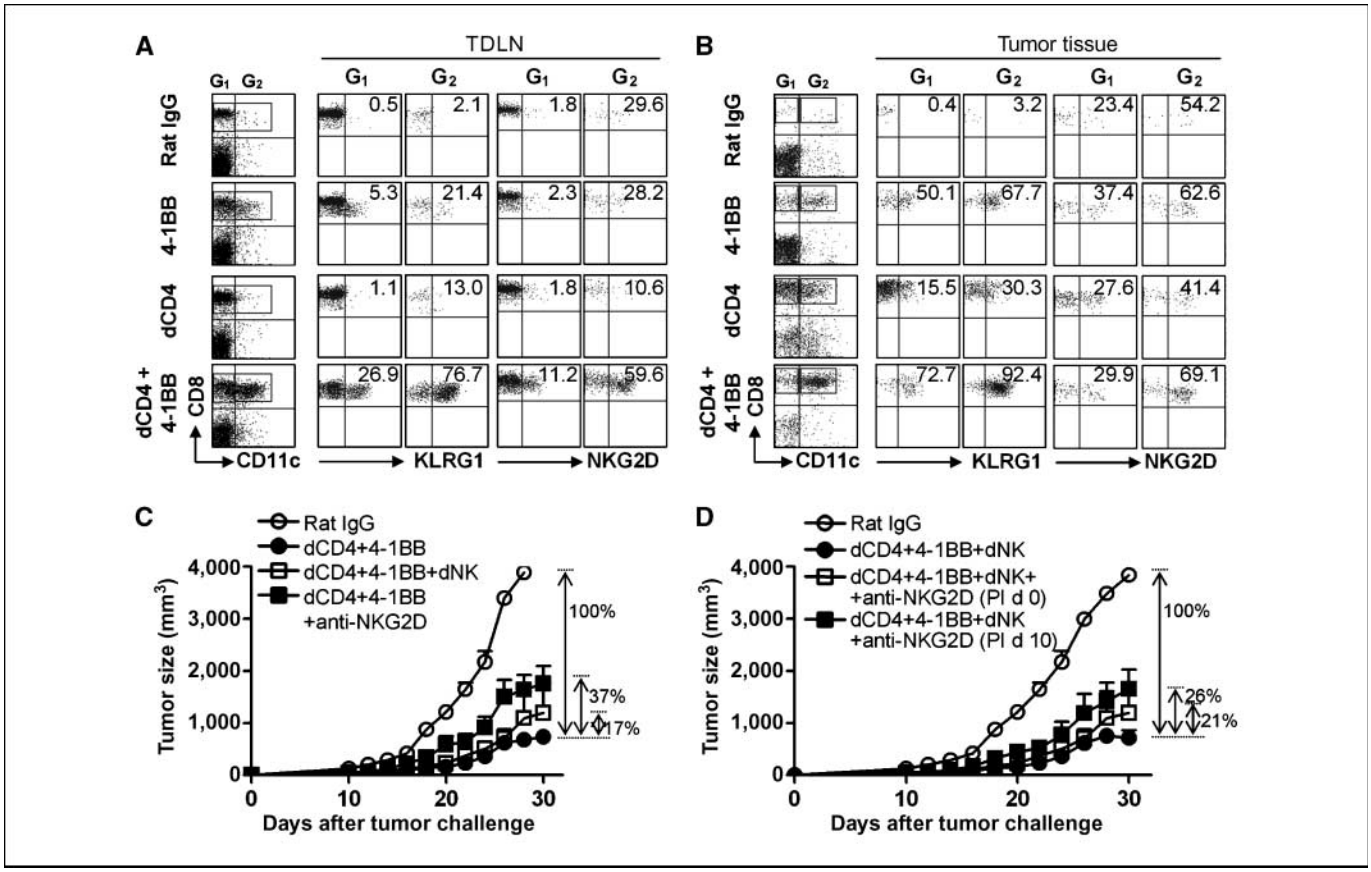

Figure 5. KLRG1$^+$NKG2D$^+$CD11c$^+$CD8$^+$ T cells become the tumor-infiltrating effector T cells of anti-4-1BB therapy. Tumor-challenged mice were treated with antibodies as described above. On PI day 15, TDLN cells (*A*) and TILs (*B*) were stained with antibodies against KLRG1 or NKG2D as well as PE-Cy5–conjugated anti-CD8 and PE-conjugated anti-CD11c mAbs. All samples were subsequently analyzed on FACS. *C,* tumor-challenged mice were treated with anti-4-1BB and/or anti-CD4, rat IgG as a control. Some mice received anti-4-1BB plus anti-CD4 mAb were further treated with 400 μg anti-NK1.1 (PK136; dNK) or 500 μg anti-NKG2D (C7) mAb from PI day 10 every 5 d. *D,* anti-4-1BB and anti-CD4–treated mice received 400 μg anti-NK1.1 mAb on PI day 10, and were also given 500 μg anti-NKG2D mAb from PI day 0 or 10 every 5 d, rat IgG as a control. The mice were monitored every day to measure the growth of tumors. *Points,* mean (n = 5 mice per group in *A* and *B* and n = 10 mice per group in *C* and *D*); *bars,* SD. All results are representative of three independent experiments.

constitute a barrier to immune cell infiltration. Even the absolute number of CD11c$^+$CD8$^+$ T cells with anti-CD4 treatment was 2-fold more than with anti-4-1BB treatment. Again, the combination therapy greatly enhanced the infiltration of CD11c$^+$CD8$^+$ T cells into tumor tissues. These were rarely found in the rat IgG-treated control mice (Fig. 4*B*).

We compared the gene expression profile of the CD11c$^+$CD8$^+$ T cells with that of the CD11c$^-$CD8$^+$ T cells in the rat IgG-treated mice by microarray analysis. Among the genes that were up- or down-regulated in the CD11c$^+$CD8$^+$ T cells (a complete analysis will be published elsewhere), *NKG2D* and *KLRG1* were highly expressed in the CD11c$^+$CD8$^+$ T cells and not present at all in the CD11c$^-$CD8$^+$ T cells.

NKG2D on the CD11c$^+$CD8$^+$ T cells is involved in tumor killing. The expression of NKG2D may mean that this receptor provide an additional armamentarium for tumor cell killing by the CD11c$^+$CD8$^+$ T cells, whereas the KLRG1-expressing CD8$^+$ T cells may represent memory or effector cells that are terminally differentiated (12). We tested for surface expression of NKG2D and KLRG1 by flow cytometry. TDLN cells from the anti-4-1BB and/or anti-CD4–treated mice were surface-stained with anti-KLRG1 or anti-NKG2D along with anti-CD11c-PE and anti-CD8β-PE-Cy5. The CD8$^+$ T cells were further divided into CD11c$^+$ and CD11c$^-$ by gating on a CD8 versus CD11c plot, and the expression of KLRG1 and NKG2D on each population was determined. KLRG1 and NKG2D were mainly expressed on the CD11c$^+$CD8$^+$ rather than the CD11c$^-$CD8$^+$ T cells (Fig. 5*A*). In the TDLNs, both KLRG1 and NKG2D were almost undetectable in the control IgG or anti-CD4–treated CD11c$^-$CD8$^+$ T cells. Their expression was, however, increased in the anti-4-1BB– or combination-treated CD11c$^-$CD8$^+$ T cells (Fig. 5*A*). Both NKG2D and KLRG1 were detected at higher levels in the CD11c$^+$CD8$^+$ T cells in all the treatment groups, the highest levels being present in the combination therapy group (76.7% and 59.6%, respectively; Fig. 5*A*). The analysis of TILs again indicated that KLRG1 and NKG2D were associated with CD11c$^+$CD8$^+$ T cells; KLRG1 was detected in 92.4% of the CD11c$^+$CD8$^+$ TILs, and NKG2D was detected in 69.1% of the CD11c$^+$CD8$^+$ TILs (Fig. 5*B*). NKG2D and KLRG1 seem to be induced by anti-4-1BB stimulation because expression of the receptors was more responsive to anti-4-1BB than to anti-CD4 (Fig. 5*B*).

We asked whether NKG2D expression contributed to the CD11c$^+$CD8$^+$ T cell–mediated antitumor responses. To accurately measure the contribution of NKG2D to CD11c$^+$CD8$^+$ T-cell activities, we first eliminated NK cells because NKG2D is expressed on both NK and CD8$^+$ T cells (13). Anti-4-1BB and anti-CD4–treated mice were given anti-NK1.1 mAb from PI day 10 because CD11c$^+$CD8$^+$ T cells began to increase 8 days after tumor challenge. The depletion of NK cells reduced antitumor effects by 17%

(Fig. 5*C*). We also depleted NK cells 1 day before the tumor challenge, and this had a similar effect to that of the delayed depletion of NK cells (data not shown). Blocking NKG2D decreased the antitumor effect by 37% (Fig. 5*C*). If we subtract the contribution of the NK cells (17%), ~20% of the antitumor effect was due to the NKG2D on the $CD8^+$ T cells. To confirm the role of NKG2D on the T cells, tumor-bearing mice were given anti-NK1.1 mAb on PI day 10 along with anti-NKG2D on PI day 0 or 10. In the absence of NK cells, blocking NKG2D decreased the antitumor effect by 21% to 26%, indicating that NKG2D is active in the $CD11c^+CD8^+$ T cell–mediated anticancer effects and contributes to 20% to 26% of the CTL activity in the tumors (Fig. 5*D*).

We have thus provided evidence that $NKG2D^+KLRG1^+CD11c^+CD8^+$ T cells preferentially infiltrate into tumor tissue and inhibit tumor growth. We conclude that the anti-4-1BB–mediated differentiation of $CD8^+$ T cells yields $NKG2D^+KLRG1^+CD11c^+CD8^+$ T cells and that their infiltration is amplified by depleting $CD4^+$ cells.

Anti-4-1BB or/and anti-CD4 change the tumor microenvironment. We next investigated possible changes of the tumor microenvironment induced by the combination therapy. We first asked whether combination therapy enhanced the expression of MHC class I molecules on the melanoma cell surfaces because effective tumor killing by $CD8^+$ T cells requires antigen presentation. The combination therapy proved very effective in inducing both $H\text{-}2K^b$ and $H\text{-}2D^b$ molecules on the melanoma cells. Expression in the combination therapy reached 88.5% for $H\text{-}2K^b$ and 98.1% for $H\text{-}2D^b$, whereas the control IgG-treated group gave only 1.5% for $H\text{-}2K^b$ and 10.1% for $H\text{-}2D^b$. Remarkably, depletion of $CD4^+$ cells was also quite effective in inducing these class I molecules on the melanomas (46.1% for $H\text{-}2K^b$ and 64% for $H\text{-}2D^b$). Anti-4-1BB alone was less effective than depletion of $CD4^+$ cells in inducing them (4.5% for $H\text{-}2K^b$ and 24.2% for $H\text{-}2D^b$; Fig. 6*A* and *C*). In view of the fact that almost all the melanoma cells express IFN-γR (Fig. 6*A*) and that class I molecule induction is almost at a basal level in IFN-γ KO (GKO) mice (Fig. 6*A, bottom*), the production of IFN-γ inside the tumors must play a major role in inducing the expression of $H\text{-}2K^b$ and $H\text{-}2D^b$.

Depletion of $CD4^+$ cells may result in the elimination of $CD4^+CD25^+$ Treg- and IDO-producing dendritic cells, which are known to suppress antitumor immunity (14–16). As expected, anti-CD4 completely depleted both $CD4^+$ effector and regulatory T cells in the TDLNs and tumor tissues (Supplementary Fig. S5*A*). Anti-CD4 depleted 50% to 70% of the plasmacytoid dendritic cells that expressed PDCA-1 (Supplementary Fig. S5*B*), and markedly reduced the number of IDO-expressing dendritic cells (Fig. 6*C*). In agreement with the these results, IDO^+ cells were readily detected in TDLN sections of the rat IgG- or anti-4-1BB–treated mice, but were barely detectable in the mice treated with anti-CD4– or anti-4-1BB plus anti-CD4 (Fig. 6*D*).

Depletion of Treg by anti-CD25 showed only mild therapeutic effect, which seemed to be due to the additional depletion of activated T cells that expressed CD25. The combination of anti-4-1BB with 1-MT had a limited therapeutic effect on B16-F10 melanoma model (Supplementary Fig. S6*A*). This may be due to the fact that 1-MT inhibits the NK activity (17). Blockade of transforming growth factor β along with anti-4-1BB definitely suppressed the tumor growth, but showed a reduced survival rate (Supplementary Fig. S6*B*).

We conclude that anti-CD4 treatment strengthens the anti-4-1BB–mediated $CD8^+$ T-cell response by inducing the formation of class I molecules on tumor cells and removing IDO^+ dendritic cells and Treg cells.

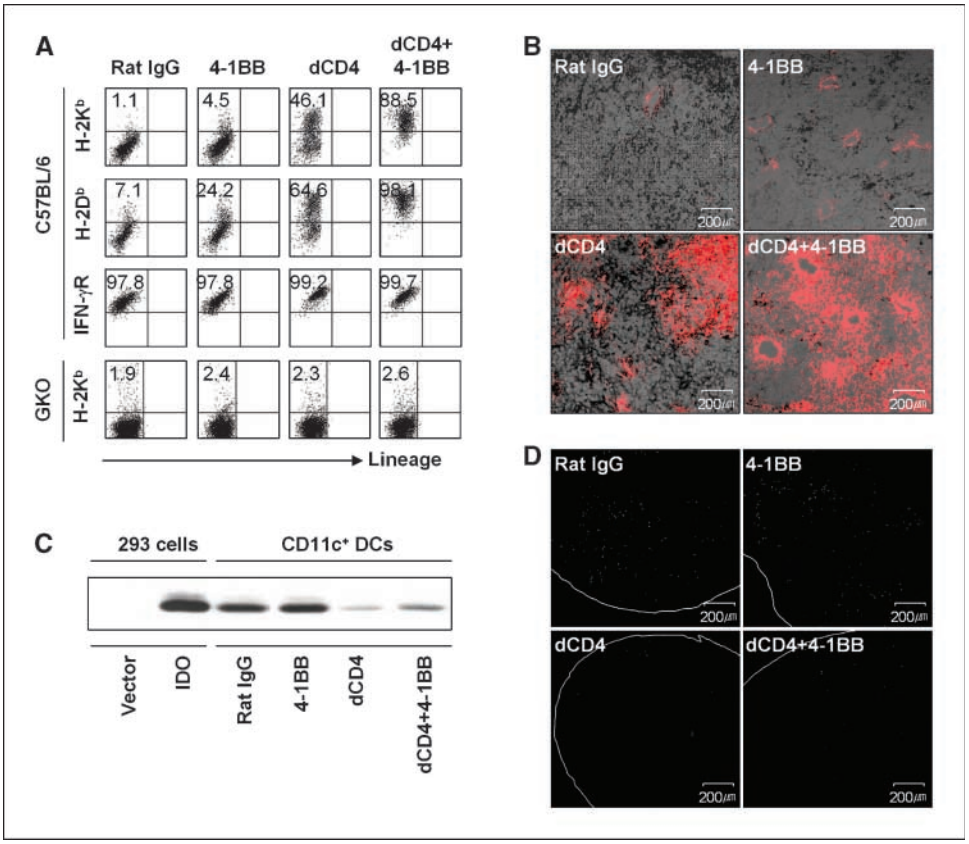

Figure 6. Combined therapy alters the tumor microenvironment to be susceptible to $CD8^+$ T cells. Tumor-bearing C57BL/6 or IFN-γ–deficient (GKO) mice were treated with 100 μg anti-4-1BB and/or 400 μg anti-CD4 mAb, and rat IgG as a control, on PI days 0, 5, and 10. *A,* tumor tissues were collected from each group of mice on PI day 15 and stained with FITC-conjugated lineage marker along with PE-conjugated anti-$H\text{-}2D^b$, $H\text{-}2K^b$, or IFN-γR. B16-F10 melanoma cells were separated by gating lineage-negative cells and analyzed for the expression of $H\text{-}2D^b$, $H\text{-}2K^b$, or IFN-γR. *B,* frozen sections (5 μm thickness) of tumor tissue were prepared from each group of mice on PI day 15 and stained with PE-conjugated anti-$H\text{-}2K^b$ mAb. *C,* TDLNs was collected from the four groups of mice on PI day 15 and digested with 0.1% collagenase and 0.2 mg/mL DNase I for 30 min. Cells were incubated with Thy1.2 microbeads and loaded on a column to deplete T cells. $CD11c^+$ dendritic cells were purified from the T cell–depleted TDLN cells using CD11c microbeads (Miltenyi Biotec), and Western blotting was done using 5 μg of cell lysates and anti-mouse IDO mAb. *D,* frozen sections (5 μm thickness) were prepared from TDLN on PI day 15 and stained with FITC-conjugated anti-IDO mAb after alcohol fixation. Sections were viewed and photographed using a laser-scanning confocal fluorescence microscope system (Fluoview FV500, original magnification, ×10). All results are representative of three independent experiments.

Discussion

4-1BB is induced on the T-cell surface in an antigen-specific manner. The 4-1BB–mediated therapeutic effect, therefore, is an antigen-driven phenomenon. 4-1BB triggering could provide the selectivity of immunotherapy and minimize adverse effects on global host immune responses. 4-1BB alone, however, has a limited therapeutic effect against highly metastatic nonimmunogenic tumors such as the B16-F10 melanoma. This limitation seems to arise from the regulatory mechanisms of the host immune system itself. When we removed some of the regulatory barriers by anti-CD4, the antitumor effect was remarkably enhanced. We have shown that all aspects of the antitumor activities were synergistically enhanced by the combination therapy: proliferation of $CD8^+$ T cells, $CD8^+$ T-cell differentiation, production of proinflammatory cytokines, expansion of polyclonal cytotoxic effectors, infiltration of effector $CD8^+$ T cells into tumor tissues, and induction of a susceptible tumor microenvironment. More importantly, these factors were translated into a synergistic antitumor effect.

The results of the present investigation deliver the strong message that the immune system contains multiple layers of $CD4^+$ cell-mediated regulatory mechanisms against $CD8^+$ T cell–mediated antitumor immunity. $CD4^+$ cells inhibited the expansion and differentiation of antitumor $CD8^+$ T cells, and blocked the infiltration of immune cells into tumor tissues (Figs. 2–4). Interestingly, depletion of $CD4^+$ cells was very effective in inducing the formation of MHC class I molecules on the tumor cells *in vivo* (Fig. 6). This phenomenon may be related to the massive infiltration of various immune cells into the tumors and the production of IFN-γ in the tumor microenvironment.

Induction of high level of IFN-γ was shown to impair $CD8^+$ T-cell memory due to the apoptosis of $CD4^+$ T cells (18). We examined a potential role of anti-4-1BB in the generation of the memory $CD8^+$ T by transferring OVA-specific $CD8^+$ T cells into $rag2^{-/-}$ mice and found that anti-4-1BB could generate the memory $CD8^+$ T cells in the absence of $CD4^+$ T cells. Anti-4-1BB–mediated induction of IL-7 and IL-15 in $CD8^+$ T cells seem to provide some of the helping functions of $CD4^+$ T cells.[5]

It was remarkable that 4-1BB stimulation alone drove the differentiation and expansion of $CD8^+$ T cells in an antigen-specific manner in the absence of $CD4^+$ T cells (Figs. 2*D* and 3*B*). This is in line with results that suggested that 4-1BB triggering provides certain signals supposed to be provided by $CD4^+$ helper T cells (19, 20). 4-1BB–dependent and antigen-driven expansion of $CD11c^+CD8^+$ T cells has been shown in herpes simplex virus-1 infection (21), autoimmune disease (2, 22), and B16 tumor models (current studies). $CD11c^+CD8^+$ T cells have dual regulatory roles: They suppress antigen-specific $CD4^+$ T cells by an IDO-dependent mechanism in autoimmune disease models (2), and they themselves become effective CTLs in viral infection and tumor models. The origin and developmental requirements of such $CD11c^+CD8^+$ regulatory T cells remain to be determined.

All the mice received the combination therapy eventually died around PI days 70 to 80. Further delay of the combination therapy provides little survival advantage in spite of enhanced $CD11c^+CD8^+$ T response in TDLNs.

Anti-4-1BB is known to induce IDO in dendritic cells and macrophages (2, 22), and this generates a barrier to tumor therapy. Removing $CD4^+$ cells eliminated ~70% of the IDO-producing cells and all the Treg cells, and this may contribute to the enhanced antitumor outcome. Yu et al. (14) showed that local depletion of $CD4^+$ cells led to the eradication of established tumor and development of long-term antitumor immunity.

Anti-4-1BB therapy has shown to be effective in various tumor models (5, 19, 23). Anti-4-1BB has been also used in combination with IL-12–expressing dendritic cell (24), human telomerase reverse transcriptase gene therapy (25), dendritic cell–based vaccine (4), IL-12 gene therapy (3), and radiation (26). Soluble 4-1BB ligand in combination with IL-12 gene therapy produced potent antitumor response against hepatic colon carcinoma model (27). Induction of potent antitumor effect by the use of single-chain Fv of anti-4-1BB is another important approach (28, 29).

NKG2D and KLRG1-positive $CD11c^+CD8^+$ T cells preferentially accumulated inside tumor tissues. Significance of KLRG-1 expression (12) remains to be determined. NKG2D may function as a costimulatory receptor or it may provide the $CD8^+$ T cells with MHC-independent killing capability (13, 30, 31), although this aspect requires further investigation of the roles of authentic ligands such as RAE-1, H60, and MULT-1 (13, 32, 33).

Current studies suggest that one single type of immunotherapy may not be able to deal with all facets of tumor progression, and tumor- and immune system–derived regulatory barriers. Therefore, a rational combination of synergistic immunotherapies could provide a successful clinical approach to human cancers. The recent treatment of melanoma by adoptive TIL transfer in nonmyeloablative lymphodepleting conditions may be another example of overcoming tumor escape mechanisms and regulatory barriers (34, 35). Considering the difficulties involved in preparing a large number of TILs *in vitro* in the adoptive therapy, new therapeutic modalities that achieve such an antitumor effect by injecting combinations of immunotherapeutics need to be developed.

[5] Unpublished results.

Acknowledgments

Received 3/20/2007; revised 5/31/2007; accepted 7/2/2007.

Grant support: NIH grants R01EY013325, KRF-2005-201-E00008, and KRF-2005-084-E00001, Innovative Research Award from Arthritis Foundation, Atlanta, GA, and Science Research Centre funds to the Immunomodulation Research Center, from Korea Science and Engineering Foundation.

The costs of publication of this article were defrayed in part by the payment of page charges. This article must therefore be hereby marked *advertisement* in accordance with 18 U.S.C. Section 1734 solely to indicate this fact.

References

1. Pollok KE, Kim YJ, Zhou Z, et al. Inducible T cell antigen 4-1BB. Analysis of expression and function. J Immunol 1993;150:771–81.
2. Seo SK, Choi JH, Kim YH, et al. 4-1BB-mediated immunotherapy of rheumatoid arthritis. Nat Med 2004;10:1088–94.
3. Xu D, Gu P, Pan PY, Li Q, Sato AI, Chen SH. NK and $CD8^+$ T cell-mediated eradication of poorly immunogenic B16-10 melanoma by the combined action of IL-12 gene therapy and 4-1BB costimulation. Int J Cancer 2004;109:499–506.
4. Ito F, Li Q, Shreiner AB, et al. Anti-CD137 monoclonal antibody administration augments the antitumor efficacy of dendritic cell-based vaccines. Cancer Res 2004;64:8411–9.
5. Kim JA, Averbook BJ, Chambers K, et al. Divergent effects of 4-1BB antibodies on antitumor immunity and on tumor-reactive T-cell generation. Cancer Res 2001;61:2031–7.
6. Ju SA, Lee SC, Kwon TH, et al. Immunity to melanoma mediated by 4-1BB is associated with enhanced activity of tumour-infiltrating lymphocytes. Immunol Cell Biol 2005;83:344–51.
7. Ho EL, Carayannopoulos LN, Poursine-Laurent J, et al. Costimulation of multiple NK cell activation receptors by NKG2D. J Immunol 2002;169:3667–75.

8. Rubio V, Stuge TB, Singh N, et al. *Ex vivo* identification, isolation and analysis of tumor-cytolytic T cells. Nat Med 2003;9:1377–82.
9. Freeman GJ, Sharpe AH, Kuchroo VK. Protect the killer: CTLs need defenses against the tumor. Nat Med 2002;8:787–9.
10. Brentjens RJ, Latouche JB, Santos E, et al. Eradication of systemic B-cell tumors by genetically targeted human T lymphocytes co-stimulated by CD80 and interleukin-15. Nat Med 2003;9:279–86.
11. Arens R, Schepers K, Nolte MA, et al. Tumor rejection induced by CD70-mediated quantitative and qualitative effects on effector $CD8^+$ T cell formation. J Exp Med 2004;199:1595–605.
12. Voehringer D, Koschella M, Pircher H. Lack of proliferative capacity of human effector and memory T cells expressing killer cell lectin like receptor G1 (KLRG1). Blood 2002;100:3698–702.
13. Markiewicz MA, Carayannopoulos LN, Naidenko OV, et al. Costimulation through NKG2D enhances murine $CD8^+$ CTL function: similarities and differences between NKG2D and CD28 costimulation. J Immunol 2005;175:2825–33.
14. Yu P, Lee Y, Liu W, et al. Intratumor depletion of $CD4^+$ cells unmasks tumor immunogenicity leading to the rejection of late-stage tumors. J Exp Med 2005;201:779–91.
15. Munn DH, Sharma MD, Hou D, et al. Expression of indoleamine 2,3-dioxygenase by plasmacytoid dendritic cells in tumor-draining lymph nodes. J Clin Invest 2004;114:280–90.
16. Shortman K, Liu YJ. Mouse and human dendritic cell subtypes. Nat Rev Immunol 2002;2:151–61.
17. Kai S, Goto S, Tahara K, et al. Inhibition of indoleamine 2,3-dioxygenase suppresses NK cell activity and accelerates tumor growth. J Exp Ther Oncol 2003;3:336–45.
18. Berner V, Liu H, Zhou Q, et al. IFN-γ mediates $CD4^+$ T-cell loss and impairs secondary antitumor responses after successful initial immunotherapy. Nat Med 2007;13:354–60.
19. May KF, Jr., Chen L, Zheng P, Liu Y. Anti-4-1BB monoclonal antibody enhances rejection of large tumor burden by promoting survival but not clonal expansion of tumor-specific $CD8^+$ T cells. Cancer Res 2002;62:3459–65.
20. Laderach D, Movassagh M, Johnson A, Mittler RS, Galy A. 4-1BB co-stimulation enhances human CD8(+) T cell priming by augmenting the proliferation and survival of effector CD8(+) T cells. Int Immunol 2002;14:1155–67.
21. Kim YH, Seo SK, Choi BK, et al. 4-1BB costimulation enhances HSV-1-specific $CD8^+$ T cell responses by the induction of $CD11c^+CD8^+$ T cells. Cell Immunol 2005;238:76–86.
22. Choi BK, Asai T, Vinay DS, Kim YH, Kwon BS. 4-1BB-mediated amelioration of experimental autoimmune uveoretinitis is caused by indoleamine 2,3-dioxygenase-dependent mechanisms. Cytokine 2006;34:233–42.
23. Wilcox RA, Flies DB, Zhu G, et al. Provision of antigen and CD137 signaling breaks immunological ignorance, promoting regression of poorly immunogenic tumors. J Clin Invest 2002;109:651–9.
24. Tirapu I, Arina A, Mazzolini G, et al. Improving efficacy of interleukin-12-transfected dendritic cells injected into murine colon cancer with anti-CD137 monoclonal antibodies and alloantigens. Int J Cancer 2004;110:51–60.
25. Lin X, Zhou C, Wang S, et al. Enhanced antitumor effect against human telomerase reverse transcriptase (hTERT) by vaccination with chemotactic-hTERT gene-modified tumor cell and the combination with anti-4-1BB monoclonal antibodies. Int J Cancer 2006;119:1886–96.
26. Shi W, Siemann DW. Augmented antitumor effects of radiation therapy by 4-1BB antibody (BMS-469492) treatment. Anticancer Res 2006;26:3445–53.
27. Xu DP, Sauter BV, Huang TG, et al. The systemic administration of Ig-4-1BB ligand in combination with IL-12 gene transfer eradicates hepatic colon carcinoma. Gene Ther 2005;12:1526–33.
28. Ye Z, Hellstrom I, Hayden-Ledbetter M, et al. Gene therapy for cancer using single-chain Fv fragments specific for 4-1BB. Nat Med 2002;8:343–8.
29. Yang Y, Yang S, Ye Z, et al. Tumor cells expressing anti-CD137 scFv induce a tumor-destructive environment. Cancer Res 2007;67:2339–44.
30. Verneris MR, Karami M, Baker J, Jayaswal A, Negrin RS. Role of NKG2D signaling in the cytotoxicity of activated and expanded $CD8^+$ T cells. Blood 2004;103:3065–72.
31. Maccalli C, Pende D, Castelli C, Mingari MC, Robbins PF, Parmiani G. NKG2D engagement of colorectal cancer-specific T cells strengthens TCR-mediated antigen stimulation and elicits TCR independent anti-tumor activity. Eur J Immunol 2003;33:2033–43.
32. Diefenbach A, Jensen ER, Jamieson AM, Raulet DH. Rae1 and H60 ligands of the NKG2D receptor stimulate tumour immunity. Nature 2001;413:165–71.
33. Carayannopoulos LN, Naidenko OV, Fremont DH, Yokoyama WM. Cutting edge: murine UL16-binding protein-like transcript 1: a newly described transcript encoding a high-affinity ligand for murine NKG2D. J Immunol 2002;169:4079–83.
34. Rosenberg SA, Dudley ME. Cancer regression in patients with metastatic melanoma after the transfer of autologous antitumor lymphocytes. Proc Natl Acad Sci U S A 2004;101:14639–45.
35. Dudley ME, Wunderlich JR, Yang JC, et al. Adoptive cell transfer therapy following non-myeloablative but lymphodepleting chemotherapy for the treatment of patients with refractory metastatic melanoma. J Clin Oncol 2005;23:2346–57.

Mechanisms Involved in Synergistic Anticancer Immunity of Anti-4-1BB and Anti-CD4 Therapy

Beom K. Choi, Young H. Kim, Woo J. Kang, et al.

Cancer Res 2007;67:8891-8899.